Atmos. Meas. Tech. Discuss., 6, 9623–9653, 2013
www.atmos-meas-tech-discuss.net/6/9623/2013/
doi:10.5194/amtd-6-9623-2013

Atmospheric Measurement Techniques Discussions

Open Access

Relationship between optical extinction and liquid water content in fogs

C. Klein and A. Dabas

Groupe d'Étude de l'Atmosphère Météorologique (GAME) – UMR3589, Unité Mixte de Recherche 3589 de Météo-France et du CNRS, Toulouse, France

Received: 27 August 2013 – Accepted: 21 September 2013 – Published: 8 November 2013

Correspondence to: A. Dabas (alain.dabas@meteo.fr)

Published by Copernicus Publications on behalf of the European Geosciences Union.

Abstract

Studies carried out in the late 1970s suggest a simple linear relationship exists in practice between the optical extinction in the thermal IR and the liquid water content (LWC) in fogs. Such a relationship opens the possibility to monitor the vertical profile of the LWC in fogs with a rather simple backscatter lidar. Little is known on how the LWC varies as a function of height and during the fog life cycle, so the new measurement technique would help understand fog physics and provide valuable data for improving the quality of fog forecasts. In the present article, the validity of the linear relationship is revisited at the light of recent observations of fog droplet size distributions measured with a combination of sensors covering a large range of droplet radii. In particular, large droplets (radius above 15 µm) are detected, which was not the case in the late 1970s. The results confirm the linear relationship still holds, at least for the mostly radiative fogs observed during the campaign. The impact of the precise value of the real and imaginary parts of the refractive index on the coefficient of the linear relationship is also studied. The usual practice considers droplets are made of pure water. This assumption is probably valid for big droplets, it may be questioned for small ones since droplets are formed from condensation nuclei of highly variable chemical composition. The study suggests the relationship is mostly sensitive to the real part of the refractive index and the sensitivity grows with the size of fog droplets. However, large fog droplets are more likely to have an index close to that of water since they are mainly composed of water.

1 Introduction

Improving the quality of fog forecasts is a challenge for weather prediction centres. Fog is indeed a common weather phenomenon with a strong, adverse impact on human activities. This is particularly true for aviation. For instance, the worst crash in the aviation history happened in 1977 in Teneriffe with the collision of two Boing 747 jumbo-jets on

AMTD
6, 9623–9653, 2013

the runaway and the death of more than 500 persons. The dense fog on the airport was a key factor (see ICAO Circular 135/AN156). Fortunately, the impact of fog on airports is not so severe most of the time, but safety regulations limit the capacity of the runaways when the visibility is too short (e.g. runway visual range less than 600 m at Paris Roissy Charles-de-Gaulle airport), leading to costly delays, missed connections, and cancellations (see Sullivan and Jordan, 2006, for a description of possible disruptions on a major airport like London Heathrow).

The cost for airports and aviation companies has led many research centres around the world to work on fog physics and fog numerical simulation. The final objective is to develop operational tools for accurate predictions of the formation and the dissipation of fog several hours in advance. If such tools were existing airports and companies could warn the passengers, encourage them to cancel their flight, and mitigate the impact by an adequate organization of the time slots still available.

Weather conditions favourable to fog formation are well known and predictable, but accurate predictions of the time of formation and dissipation is presently an unmet challenge. The reason is fog is a local phenomenon with a small vertical extension (several hundreds of meters at worst) and it involves several small-scale, highly non-linear processes. These processes are not always fully understood and they are anyway all difficult to represent in numerical models (a complete review of the state of the art in fog physics can be found in Gultepe, 2007). Such processes include e. g. radiative transfer, turbulence, activation of aerosols into water drops . . .

Several directions are currently pursued for improving our understanding of fog and ultimately its forecast. One of them deals with the observation. Current observation systems provide useful information but are operated at the ground and characterize the state of the atmosphere in the lowest meters and not above. Observation systems for altitude measurements used operationally or for research are ill adapted. Research aircrafts for instance cannot fly in fogs as these are thin – they would have to fly close to the ground – while the visibility is weak. Instrumented masts are possible, but are expensive and are deployed with difficulty close to airfields. Free or tethered balloons are another possibility, but they are "single shot" (free balloons) or imply complex operations that limit their practical usefulness (Dabas et al., 2012). Remote sensors would offer many advantages. Deployed at ground, they can be operated unattended for long periods of time. As an instance, Paris Charles-de-Gaulle airport has been equipped with a sodar since 2008. It detects the top height of fog layers and provides this information to the operational fog prediction system COBEL (Dabas et al., 2012; Bergot and Guédalia, 1994).

The work reported in the present article is part of an effort aimed at developing a lidar able to measure vertical profiles of the liquid water content (LWC). The LWC can be measured at ground (Gerber, 1991), but altitude measurements are scarce because they are difficult to achieve with current sensors. Observations are thus lacking for validating model simulations (Bergot, 2013). Besides, real time LWC observation could have a significant impact on fog predictions (Remy and Bergot, 2009). In this article, the possibility to measure the LWC with a lidar is based on the existence of a relationship between the LWC and the optical extinction in fogs. Such a relationship was postulated by Chylek (1978) in the late 1970s and tested experimentally by Pinnick et al. (1979) in the same period. In principle, lidars can measure extinction coefficients. Due to the strong optical extinction in fogs their range is limited but fogs are thin (a few tens to a few hundreds of meters) so it should be possible to obtain useful measurements.

The experimental validation of Pinnick et al. (1979) was based on a particle counter and sizer developed by the Particle Measurement Systems Inc. in the 1970s. The sensor is described in Pinnick et al. (1978). According to the article, a major limitation was that particles with radii $> 15\,\mu m$ were only partially detected due to losses in the ventilated collection tube. Thus the impact of larger droplets in fogs, if any, could not be evaluated. A second limitation was that extinction coefficients were computed using the Mie theory with refraction indices of pure water. The refraction index of large droplets is probably close to pure water because they mostly contain water. However, drops are formed from condensation nuclei, that is, aerosols. Their refraction index depends on their chemical composition (Fenn et al., 1985; Guyon et al., 2003). In fogs,

AMTD
6, 9623–9653, 2013

many droplets are small with diameters of the order of a micron or less. They contribute significantly to the extinction through scattering. The relative contribution of their condensation nucleus to their chemical composition might not be negligible and impact their refraction index.

The purpose of the present paper is twofold. First, Pinnick et al. results are revisited on the basis of observations carried out recently with a state-of-the art instrumental setup. Described in Sect. 2, the setup can in principle detect and size fog droplets up to a diameter of 50 µm. In Sect. 3, the linear relationship between optical extinction and LWC in fogs is checked. Then (Sect. 4) the potential impact of the refractive index is studied. As there are very few measurements of the refractive index of fog droplets, the study determines how far indices can deviate from pure water before the extinction to LWC relationship is significantly impacted. Conclusions are drawn in Sect. 5.

2 Experimental setup and data

The size distributions used in this article were measured during a field experiment called ParisFog (Haeffelin et al., 2010) in the frame of the research study PREVIBOSS (Elias et al., 2012). This study was designed to improve the understanding of processes involved in the life cycle of fog. It was held at Site Instrumental de Recherche en Télédétection Atmosphérique (SIRTA) located 25 km south of Paris (Heaffelin et al., 2005). Data were monitored during the winters 2010/2011 and 2011/2012. Aerosol and fog particles size distributions were measured with two instruments: a Welas-2000, and a Fog Monitor 100 (Burnet et al., 2012).

Manufactured by PALAS, the Welas 2000 measures the concentration and size of particles by looking at the 90° scattering of a white light source. The size range depends on instrumental settings and type of particles. During PARISFOG, the system was expected to measure water particles from diameters of 0.4 µm to about 20 µm. The instrument was 3 m above the ground.

Discussion Paper | Discussion Paper | Discussion Paper | Discussion Paper |

AMTD

6, 9623–9653, 2013

Relationship between optical extinction and liquid water content in fogs

C. Klein and A. Dabas

The FM100 is manufactured by *Droplet Measurement Technologies* (DMT). It is a forward scattering spectrometer probe placed in a wind tunnel with active ventilation. The FM100 detects particles in the diameter range 2 to 50 µm. The size distributions used in this article are retrieved with the manufacturer's software delivered with the FM100. The actual performances of the FM100 are discussed in Spiegel et al. (2012).

The WELAS and the FM100 are complementary sensors. The WELAS measures small particles (up to a few microns), and the FM100 the large ones (up to several tens of microns). Intermediate sizes are detected by both so the consistency of their size distributions can be checked. Both instruments were calibrated before the campaigns with glass or latex beads, but the estimation of detected droplets is done with a calibration curve that assumes the droplets are made of water. Note that the droplet size distributions used here do not need to be "real", but realistic, with regards in particular to the presence and relative contribution to LWC of large droplets.

Composite size distributions from both instruments were built and fitted with the sum of M log-normal modes

$$n(r) = \frac{1}{\sqrt{2\pi}r} \sum_{k=1}^{M} \frac{N_k}{\ln(\sigma_k)} \exp\left[-\frac{1}{2\ln^2(\sigma_k)} \ln\left(\frac{r}{r_k}\right)^2\right]. \quad (1)$$

Here, r_k is the modal radius, σ_k sets the width of the mode, and N_k the concentration of the mode. In practice, we used a maximum of $M = 4$ modes.

The following sections are based on 20 different size distributions selected among several hundreds of size distributions observed during PARISFOG. The selection was done so as to cover a large variety of fog and pre fog conditions (type, optical thickness, development stage ...). The log-normal mode characteristics are given in Table 1. They were manually fitted to the measured size distributions. A fit example is shown in Fig. 1. There the number of particles counted in the various classes of the FM100 and WELAS 2000 are displayed with blue dots. The fit with the sum of four log-normal modes is represented with a red, solid line. The individual modes are indicated with green dashes. The size distribution was observed on 19 November 2010, at 05:40 UTC

AMTD
6, 9623–9653, 2013

(06:40 LST). A mode of large particles is detected. Its modal radius is 7.5 µm (diameter 15 µm). The figure confirms the ability of the FM100 to detect and count large particles. In the present example, droplets with diameters > 15 µm are indeed detected. Although their number is small, their contribution to the overall LWC is large (more than 70 % in the present case).

3 LWC vs. extinction

The liquid water content is given by the third-order moment of the size distribution

$$W = \frac{4\pi\rho_{H_2O}}{3} \int_0^{+\infty} r^3 n(r)\mathrm{d}r \qquad (2)$$

where $\rho_{H_2O} = 1000\,\mathrm{kg\,m^{-3}}$ is the density of water. As for the extinction coefficients, we have

$$\alpha(\lambda) = \pi \int_0^{+\infty} r^2 Q_{ext}(r,\lambda) n(r)\mathrm{d}r \qquad (3)$$

with $Q_{ext}(r,\lambda)$ the extinction efficiency of the particles of radius r at the wavelength λ.

In 1978, Chylek suggested that the extinction efficiency can be reasonably well approximated by a linear relationship

$$Q_{ext}(r,\lambda) \approx c_e(\lambda)\frac{2\pi r}{\lambda} \qquad (4)$$

over the range of radii r practically found in fogs and for a well-chosen wavelength. Values for $c_e(\lambda)$ were proposed later by Pinnick et al. (1979).

AMTD
6, 9623–9653, 2013

Combining Eqs. (3) and (4), it appears the liquid water content W can be related to the extinction coefficient $\alpha(\lambda)$ through a simple, linear equation independent of the actual size distribution $n(r)$ that is thus valid for any fog

$$\hat{W} \approx \frac{2\lambda\rho_{H_2O}}{3\pi c_e(\lambda)}\alpha(\lambda). \quad (5)$$

Using Eqs. (2) and (3), the liquid water contents and extinction coefficients of the 20 selected size distributions were derived for the wavelengths λ studied in Pinnick et al. (1979). The extinction efficiency $Q_{ext}(r,\lambda)$ was computed using an adaption to the programming language SCILAB of a MATLAB code published by Mätzler (2002) (this latter one derived from Borhen and Huffman, 1983). A refractive index equal to that of pure water was considered. Its value as a function of the wavelength λ was taken from Hale and Querry (1973) (1.351 + i0.00460 @ λ = 4 µm and 1.153 + i0.0968 @ λ = 11 µm).

The 20 PARISFOG size distributions vary from weak to strong fogs (extinction coefficients from $7.8 \times 10^{-6}\,m^{-1}$ to $1.36 \times 10^{-2}\,m^{-1}$ at 11 µm, and W from $6.89 \times 10^{-5}\,g\,m^{-3}$ to $1.29 \times 10^{-1}\,g\,m^{-3}$ – see Table 1). They encompass the values considered by Pinnick et al. (1979).

The extinction coefficients and liquid water contents of the 20 fog cases are shown with grey dots on Figs. 2 and 3 for the laser wavelengths of 4 µm and 11 µm, respectively. The black curve and diamonds represent Eq. (5) (c_e(4 µm) = 0.64; c_e(11 µm) = 0.31). The results are similar to those of Pinnick et al. (1979). At λ = 4 µm, the dots are off the black line and dispersed. There seems to be no particular relationship between both parameters independent of the size distribution. At λ = 11 µm however, the dots are on the black curve suggesting the linear approximation holds. As several size distributions include a significant fraction of large droplets, Pinnick's linear approximation Eq. (5) appears to be still applicable in practice.

AMTD
6, 9623–9653, 2013

In Figs. 4 and 5 are drawn the two functions

$$F(r) = \frac{4\pi}{3} \rho_{H_2O} r^3 \tag{6}$$

and

$$\hat{F}(r) = \frac{4\rho_{H_2O}}{3c_e(\lambda)} r^2 Q_{ext}(r,\lambda). \tag{7}$$

These functions characterize the "sensitivity" of W and $\hat{W}$ to particles of radius r since

$$W = \int_0^{+\infty} F(r) n(r) dr \tag{8}$$

and

$$\hat{W} = \int_0^{+\infty} \hat{F}(r) n(r) dr. \tag{9}$$

They are drawn for $\lambda = 4\,\mu m$ (Fig. 4) and $\lambda = 11\,\mu m$ (Fig. 5), and the relative difference $\left|1 - \hat{F}/F\right|$ is displayed for both wavelengths in Figs. 6 and 7. At $4\,\mu m$, $\hat{W}$ is a poor approximation to W except for particles in the range $[2\,\mu m, 4\,\mu m]$. Outside this interval, the contribution of the particles to the liquid water content is grossly underestimated. At $11\,\mu m$, the approximation is much better and holds for particles in a much wider range. The relative error is less than 10 % for radii between $1.7\,\mu m$ and $13.2\,\mu m$. This result is noticeable as observations suggest a vast majority of fogs contain particles within this range. Larger particles may be found, but are in very small numbers and therefore shall not contribute much to the total liquid water content. Fog extinction coefficients thus seem to be an accurate proxy for their liquid water content.

AMTD
6, 9623–9653, 2013

4 Impact of the refractive index

As already mentioned, the results above are all based on extinction efficiencies calculated with the refractive index of water, that is, assuming fog particles mainly consist of water. This assumption is common in fog models or fog studies (Dumont, 2000; Elias et al., 2009; Rangognio et al., 2009; Khain et al., 2004; Laven, 2011). However, fog particles are formed from condensation nuclei, that is, aerosol, which refractive index depends on its chemical composition and can vary a lot. In large fog particles, the amount of water is large and the use of the refractive index of water is probably justified. But fogs contain small particles in large numbers, and the relative contribution of the nucleus in the overall matter of the particle may not be negligible. This is why we have studied the impact of the value of the refractive index on the W vs. extinction relationship. To our knowledge, there are no measurements of the refractive index of fog particles in the literature, so the interval of variation of the index, if any, is not known. Consequently, we did not try to see if real fluctuations of the refractive index of fog particles may or may not have an impact of how W relates to the extinction, but rather tried to determine the interval of variations the refractive index may have before it has a significant impact. We leave it to future studies to determine whether real refractive indices are within this interval or exceed it.

We proceeded in three steps. First, keeping the real value of the refractive index, we modified the imaginary part by default or excess until we found a significant impact on the extinction coefficients of the 20 PARISFOG size distributions. Second, we did the same keeping this time the imaginary part constant and tuning the real part. At last, we made the assumption that particles with a diameter larger than 1 µm are mainly made of water (the extinction coefficient for these particles is computed with the refractive index of water), and smaller particles of another matter. We considered several possible matters commonly found in aerosols and their corresponding refractive index (see Table 2 from Fenn et al., 1985).

AMTD
6, 9623–9653, 2013

Figure 8 shows how the relationship between extinction and LWC varies as a function of the imaginary part of the refractive index. The extinction computed with the index of water (cross) is the reference. Two indices have larger imaginary parts (filled circle and filled square), and two are smaller (open circle and square). The way these values were obtained is explained in Fig. 9. In the top panel are drawn the extinction efficiencies for $m = 1.153 + i0.0968$ (water – the reference), $m = 1.153 + i0.129$ (filled square in Fig. 8) and $m = 1.153 + i0.077$ (open square in Fig. 8). The latter is below the water index, the former is above, but we see in the bottom panel that both produce a maximal relative difference of 25 % with respect to water. The other indices in Fig. 8 (filled and open circles) were selected because they produce absolute relative errors of 10 %. In Fig. 8, we can see that the extinction coefficients grow when the imaginary part of the index is above water and diminish when it is below. The reason is simple: the absorption (which dominates the extinction) grows with the imaginary part of the index. The impact of the value of the imaginary part of the index is more pronounced when the LWC is small. The explanation for this is given in Fig. 9. There we can see that the relative difference of Q_{ext} to pure water is larger for radii less than 10 µm than above. Fogs with small LWC are mainly formed by small particles.

The impact of the real part of the refractive index is studied in Figs. 10 and 11. The refractive indices considered for the curves in Fig. 10 were chosen so as to produce a maximum relative difference with pure water of 10 % (circles) and 25 % (squares). The impact on the extinction coefficients are of the same order as in Fig. 8, but this time the relative variation in the index is about 5 times smaller. It thus appears here that extinction coefficients are more sensitive to the real part of the refractive index than the imaginary part. The most striking feature is that the sensitivity to the real part of the index is growing with the LWC. The reason is explained in Fig. 11. There we can see that the relative difference of Q_{ext} is maximum for radii of the order of 10 µm and remains large for radii up to 20 µm. For small radii, the relative difference grows steadily with the radius, but it is less than 5 % up to a radius of ∼ 2 µm. Light fogs with small particles are thus less affected.

AMTD
6, 9623–9653, 2013

In Fig. 12, the extinction coefficients are computed with a refractive index of several aerosol types for radii less than 1 µm (filled circles) and compared to reference extinction coefficients obtained with the refractive index of pure water for all radii (open diamonds). The wavelength is 11 µm. The values of refractive index are from Fenn et al. (1985). As it can be expected, fogs with heavy LWC are not affected by the value of the refractive index as they are formed by large particles. The impact of the refractive index is visible when the LWC is light, that is, when particles are small. The extinction coefficient may vary over at least one decade depending on which type of aerosol is chosen. For very weak LWCs, this is not a real limitation as these correspond to hazes or fogs in a very early stage of formation. However, the curves show the impact of the aerosol type can still be visible with LWCs as high as 0.01 $g\,cm^{-3}$. For these, it thus appears that the precise knowledge of the aerosol type forming cloud droplets is needed in order to make useful LWC measurements.

5 Conclusions

The study reported in the present article showed Pinnick's results published in the late 1970s are still valid when fog size distributions contain large droplets. At $\lambda = 11$ µm, the proportionality between the extinction coefficient and the LWC seems to be verified, the linear approximation of the extinction efficiency being good for droplet radii as large as 14 µm. The result is based on a limited number of fog cases, all of them obtained on the same experimental site where fogs are mostly caused by radiative cooling at the surface. On this site, the results suggest fog droplets with larger radii are scarce and do not contribute significantly to the overall LWC. It remains to be verified that this is still true for other fog types in other places. If that is so, Pinnick's linear approximation of the extinction efficiency opens a real possibility to measure vertical profiles of the LWC in fogs with a rather simple backscatter lidar operation in the thermal infrared. The size and power of such a lidar is not discussed here and left for a future publication. Preliminary studies on the subject suggest a maximum range of several hundreds of

AMTD
6, 9623–9653, 2013

meters should be possible with commercial CO_2 lasers. This range is comparable to the typical vertical extension of fogs so a profiling of the LWC through the entire fog thickness seems to be possible.

The major limitation found in the article is due to a possible uncertainty on the refractive index of particles detected by the lidar. Small particles contain a significant fraction of aerosol matter with a refractive index that may differ significantly from water. Our study suggests that thick fogs with heavy LWC are unlikely to be affected, but thin fogs may be. For these fogs, it seems that LCW measurement is mostly sensitive to the real part of the refractive index.

Acknowledgements. The data used in this article were measured on the SIRTA site in the frame of the research programme PREVIBOSS. The authors thank the SIRTA team for the provision of data and GAME colleagues Frédéric BURNET and Thierry BOURRIANE who helped select interesting fog cases, processed raw Welas and FM100 data into composite size distributions, and answered many questions about size distribution sensors and size distributions in fogs. The works reported was supported by the *Délégation Générale pour l'Armement* (French armament agency).

The publication of this article is financed by CNRS-INSU.

References

Bergot, T: Small-scale structure of radiation fog: a large-eddy simulation study, Q. J. Roy. Meteorol. Soc., 139, 1099–1112, doi:10.1002/qj.2051, 2013.

Bergot, T. and Guédalia, D.: Numerical forecasting of radiation fog, Part 1: Numerical model and sensitivity tests, Mon. Weather Rev., 122, 1218–1230, 1994.

AMTD

6, 9623–9653, 2013

Bohren, C. F. and Huffman, D. R.: Absorption and Scattering of Light by Small Particles, Wiley Interscience, New York, USA, 1983.

Burnet, F., Gomes, L., Haeffelin, M., Dupont, J.-C., and Elias, T.: Analysis of the microphysical structures of fog during the PARISFOG project, Proceedings of 16th International Conference on Clouds and Precipitation, July 2012, Leipzig, Germany, 2012.

Chylek, P.: Extinction and liquid water content of fogs and clouds, J. Atmos. Sci., 35, 296–300, 1978.

Dabas, A., Remy, S., and Bergot, T.: Use of a sodar to improve the forecast of fogs and low level clouds on airports, Pure Appl. Geophys., 169, 769–781, doi:10.1007/s00024-011-0334-y, 2012.

Dumont, E.: Caractérisation, modélisation et simulation des effets visuels du brouillard pour l'usager de la route, Ph.D. Thesis, Paris V René Descartes University, Paris, 2002.

Elias, T., Haeffelin, M., Drobinksi, P., Gomes, L., Rangognio, J., Bergot, T., Chazette, P., Raut, J.-C., and Colomb, M.: Particulate contribution to extinction of visible radiation: pollution, haze, and fog, Atmos. Res., 92, 443–454, doi:10.1016/j.atmosres.2009.01.006, 2009.

Elias, T., Jolivet, D., Dupont, J.-C., Haeffelin, M., and Burnet, F.: Preliminary results of the Pre-ViBOSS project: description of the fog life cycle by ground based and satellite observation, SPIE Proc. Ser., 8534, 853406, doi:10.1117/12.974709, 2012.

Fenn, R. W., Clough, S. A., Gallery, W. O., Goods, R. E., Kneizys, F. X., Mill, J. D., Rothmann, L. S., Shettle, E. P., and Voltz, F. E.: Optical and infrared properties of the atmosphere, in: Handbook of Geophysics and the Space Environment, 4th Edn., edited by: Jursa, A. S., Air Force Geophysics Laboratory, copies can be found at Air Force Geophysics Laboratory (SULR), Hanscom, AFB, Massachusetts, 1023 pp., 1985.

Gerber, H.: Direct measurement of suspended particulate volume concentration and far-infrared extinction coefficient with a laser-diffraction instrument, Appl. Optics, 30, 4824–4831, 1991.

Gultepe, I.: Fog and boundary layer clouds: fog visibility and forecasting, Birkhäuser, Basel, 1421 pp., 2007.

Guyon, P., Boucher, O., Graham, B., Beck, J., Mayol-Bracero, O. L., Roberts, G. C., Meanhaut, W., Artaxo, P., and Andreae, M. O.: Refractive index of aerosol particles over the Amazon tropical forest during LBA-EUSTACH 1999, Aerosol Sci., 34, 883–907, doi:10.1016/S0021-8502(03)00052-1, 2003.

Haeffelin, M., Barthès, L., Bock, O., Boitel, C., Bony, S., Bouniol, D., Chepfer, H., Chiriaco, M., Cuesta, J., Delanoë, J., Drobinski, P., Dufresne, J.-L., Flamant, C., Grall, M., Hodzic, A., Hourdin, F., Lapouge, F., Lemaître, Y., Mathieu, A., Morille, Y., Naud, C., Noël, V., O'Hirok, W., Pelon, J., Pietras, C., Protat, A., Romand, B., Scialom, G., and Vautard, R.: SIRTA, a ground-based atmospheric observatory for cloud and aerosol research, Ann. Geophys., 23, 253–275, doi:10.5194/angeo-23-253-2005, 2005.

Haeffelin, M., Bergot, T., Elias, T., Tardif, R., Carrer, D., Chazette, P., Colomb, M., Drobinski, P., Dupont, E., Dupont, J.-C., Gomes, L., Musson-Genon, L., Pietras, C., Plana-Fattori, A., Protat, A., Rangognio, J., Raut, J.-C., Rémy, S., Richard, D., Sciare, J., and Zhang, X.: PARISFOG shedding new light on fog physical processes, B. Am. Meteorol. Soc., 91, 767–783, doi:10.1175/2009BAMS2671.1, 2010.

Hale, G. M. and Querry, M. R.: Optical constants of water in the 200 nm to 200 µm wavelength region, Appl. Optics, 12, 555–563, 1973.

ICAO Circular 135/AN156: Final report and comments from the Netherlands aviation safety board of the investigation into the accident with the collision of KLM flight 4805, Boing 747-206B, PH-BUF and Pan American flight 1736, Boing 747-12; N736PA at Tenerife airport, Spain, on 27 March 1977.

Khain, A., Arkhipov, V., Pinsky, M., Feldman, Y., and Ryabov, Y. A.: Rain enhancement and fog ilimination by seeding with charged droplets, Part 1: Theory and numerical simulations, J. Appl. Meteorol., 43, 1513–1529, 2004.

Laven, P.: Time domain analysis of scattering by a water droplet, Appl. Optics, 50, 29–38, 2011.

Mätzler, C.: MATLAB functions for Mie scattering and absorption version 2, Research Report No. 2002-11, Institute of Applied Physics, University of Bern, 2002.

Pinnick, R. G., Hoihjelle, D. L., Fernandez, G., Stenmark, E. B., Lindberg, J. D., Hoidale, G. B., and Jennings, S. G.: Vertical structure in atmospheric fog and haze and its effects on visible and infrared extinction, J. Atmos. Sci., 35, 2020–2032, 1978.

Pinnick, R. G., Jennings, S. G., Chylek, P., and Auvermann, H. J.: Verification of a linear relation between IR extinction, absorption and liquid water content of fog, J. Atmos. Sci., 36, 1577–1586, 1979.

Rangognio, J.: Impact des aérosols sur le cycle de vie du brouillard, Ph.D. Thesis, Toulouse III Paul Sabatier University, Toulouse, 2009.

Rémy, S. and Bergot, T.: Assessing the impact of observations on a local numerical fog prediction system, Q. J. Roy. Meteorol. Soc., 135, 1248–1265, doi:10.1002/qj.448, 2009.

AMTD

6, 9623–9653, 2013

Relationship between optical extinction and liquid water content in fogs

C. Klein and A. Dabas

Spiegel, J. K., Zieger, P., Bukowiecki, N., Hammer, E., Weingartner, E., and Eugster, W.: Evaluating the capabilities and uncertainties of droplet measurements for the fog droplet spectrometer (FM-100), Atmos. Meas. Tech., 5, 2237–2260, doi:10.5194/amt-5-2237-2012, 2012.

Sullivan, K. and Jordan, M.: Travelers slowed, stranded as dense fog cloaks London, The Washingiton Post, Friday, 22 December 2006, available at: http://www.washingtonpost.com/wp-dyn/content/article/2006/12/21/AR2006122101535.html (last access: 31 October 2013), 2006.

Discussion Paper | Discussion Paper | Discussion Paper | Discussion Paper |

AMTD

6, 9623–9653, 2013

Relationship between optical extinction and liquid water content in fogs

C. Klein and A. Dabas

Table 1. Log-normal modes characteristics of the 20 fog size distributions used in this article. D_k is the modal diameter (equal to $2r_k$).

#	Date	Time (UTC)	Mode	N_k (part cc^{-1})	σ_k	D_k (µm)	LWC (g m^{-3})	$\lambda = 11$ µm σ_{ext} (m^{-1})	$\lambda = 11$ µm σ_{abs} (m^{-1})	$\lambda = 4$ µm σ_{ext} (m^{-1})	$\lambda = 4$ µm σ_{abs} (m^{-1})
1	19 Nov 2010	03:00	1	44	1.3	0.92	6.89E-05	7.80E-06	7.40E-06	2.70E-05	1.30E-06
			2	7	1.5	1.8					
2	16 Nov 2010	21:00	1	200	1.3	0.95	1.76E-04	1.89E-05	1.86E-05	3.41E-05	2.80E-06
			2	15	1.2	1.8					
3	16 Nov 2011	00:52	1	225	1.3	0.88	1.88E-04	2.01E-05	1.99E-05	3.12E-05	3.00E-06
			2	50	1.3	1.3					
4	16 Nov 2011	00:57	1	275	1.28	0.85	3.15E-04	3.40E-05	3.34E-05	6.72E-05	5.20E-06
			2	95	1.25	1.35					
			3	7	1.2	2.2					
5	19 Nov 2010	05:00	1	250	1.33	1.08	3.66E-04	4.06E-05	3.90E-05	1.18E-04	6.40E-06
			2	20	1.5	1.8					
6	16 Nov 2011	01:02	1	320	1.28	0.88	1.17E-03	1.50E-04	1.18E-04	6.26E-04	2.47E-05
			2	95	1.25	1.3					
			3	5	1.2	2.2					
			4	5	1.35	6					
7	16 Nov 2010	22:00	1	830	1.34	1.1	2.62E-03	2.92E-04	2.81E-04	1.13E-03	4.95E-05
			2	160	1.23	1.9					
			3	70	1.4	2.5					
8	16 Nov 2011	01:07	1	280	1.28	0.85	7.63E-03	1.02E-03	6.64E-04	2.83E-03	1.68E-04
			2	250	1.3	1.28					
			3	20	1.2	2.3					
			4	18	1.6	6.5					
9	16 Nov 2010	22:00	1	875	1.35	1.1	9.72E-03	1.25E-03	9.58E-04	5.09E-03	2.09E-04
			2	200	1.3	2					
			3	100	1.55	2.4					
			4	50	1.7	4					
10	19 Nov 2010	05:40	1	295	1.39	1.3	2.64E-02	2.87E-03	1.57E-03	4.86E-03	5.01E-04
			2	85	1.4	2.2					
			3	12	1.25	5.4					
			4	5	1.6	15					

AMTD
6, 9623–9653, 2013

Table 1. Continued.

#	Date	Time (UTC)	Mode	N_k (part cc^{-1})	σ_k	D_k (µm)	LWC (g m^{-3})	λ = 11 µm σ_{ext} (m^{-1})	λ = 11 µm σ_{abs} (m^{-1})	λ = 4 µm σ_{ext} (m^{-1})	λ = 4 µm σ_{abs} (m^{-1})
11	16 Nov 2011	01:12	1	500	1.28	0.89	5.57E-02	5.57E-03	3.07E-03	9.37E-03	1.01E-03
			2	350	1.3	1.5					
			3	20	1.18	2.8					
			4	60	2.3	4.4					
12	19 Nov 2010	06:50	1	170	1.39	1.3	4.72E-02	6.14E-03	3.53E-03	1.23E-02	1.01E-03
			2	85	1.45	2.18					
			3	42	1.39	4.88					
			4	22	1.45	12.5					
13	16 Nov 2011	01:17	1	490	1.3	0.9	5.44E-02	7.06E-03	4.08E-03	1.32E-02	1.16E-03
			2	475	1.4	1.55					
			3	45	1.5	3.1					
			4	35	1.5	11					
14	16 Nov 2011	09:22	1	865	1.33	1	5.77E-02	7.87E-03	5.18E-03	2.34E-02	1.30E-03
			2	700	1.38	1.6					
			3	195	1.55	4.5					
			4	30	1.3	11.5					
15	16 Nov 2011	01:27	1	535	1.31	0.9	6.59E-02	8.73E-03	5.21E-03	1.86E-02	1.44E-03
			2	510	1.4	1.56					
			3	95	1.6	3					
			4	55	1.5	10					
16	16 Nov 2011	08:15	1	315	1.35	1	6.71E-02	9.25E-03	5.87E-03	2.48E-02	1.52E-03
			2	300	1.38	1.62					
			3	145	1.6	5					
			4	40	1.3	11.2					
17	16 Nov 2011	05:47	1	210	1.35	1.03	9.04E-02	1.24E-02	7.56E-03	2.90E-02	2.03E-03
			2	290	1.55	1.9					
			3	70	1.28	5.6					
			4	70	1.35	11.3					
18	16 Nov 2011	04:42	1	235	1.4	1.06	9.22E-02	1.26E-02	7.65E-03	2.81E-02	2.07E-03
			2	245	1.45	1.75					
			3	80	1.6	5					
			4	68	1.36	11.2					
19	16 Nov 2010	23:00	1	1150	1.34	1.07	1.29E-01	1.31E-02	7.28E-03	2.28E-02	2.37E-03
			2	350	1.32	2					
			3	80	2	3					
			4	80	2.15	6					
20	17 Nov 2010	00:10	1	330	1.34	1.07	1.25E-01	1.36E-02	7.18E-03	2.05E-02	2.39E-03
			2	230	1.44	2					
			3	25	1.3	6.3					
			4	25	1.6	15					

AMTD
6, 9623–9653, 2013

Table 2. Refraction index of different aerosol types. From Fenn et al. (1985).

Sea salt	$1.48 + 1.4 \times 10^{-2}i$
Oceanic	$1.246 + 7.31 \times 10^{-2}i$
Ice	$1.093 + 0.239i$
Meteoric	$1.509 + 0.691i$
Water Soluble	$1.72 + 5.0 \times 10^{-2}i$
Dust	$1.62 + 0.105i$
Soot	$2.23 + 0.73i$
75 % H_2SO_4	$1.670 + 0.485i$
Volcanic	$2.15 + 0.270i$

AMTD

6, 9623–9653, 2013

Relationship between optical extinction and liquid water content in fogs

C. Klein and A. Dabas

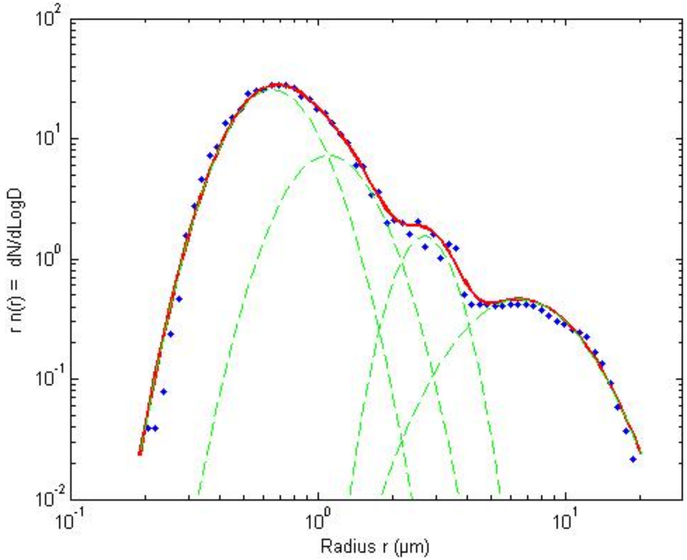

Fig. 1. Composite size distribution measured by Welas 2000 and FM100 on the 19 November 2010, at 05:40 UTC. The measurements (in parts by cubic meter and unit of natural logarithm of the diameter D) are the blue dots. A sum of $M = 4$ log-normal modes are fitted. Each mode is represented by green dashes. The sum fitted to the measurements is the red, solid, line. The parameters of the modes are given in Table 1 (fog case 10).

AMTD
6, 9623–9653, 2013

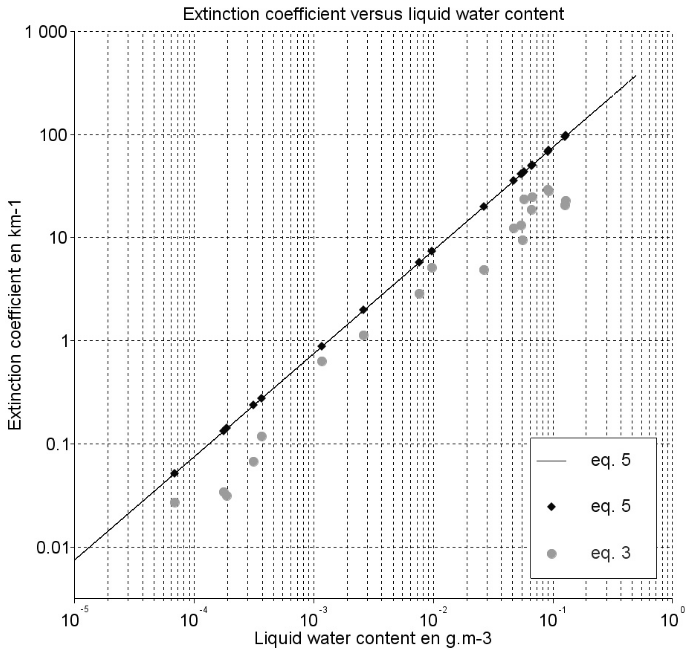

Fig. 2. Extinction coefficients at $\lambda = 4\,\mu m$ vs. the liquid water content for the 20 droplet size distributions studied in the paper. The liquid water contents are derived from the size distributions with Eq. (2). The grey dots are the extinction coefficients computed with Eq. (3) while the back curves and the diamonds show the extinction coefficients produced by the linear approximation proposed by Pinnick et al. (1979).

AMTD
6, 9623–9653, 2013

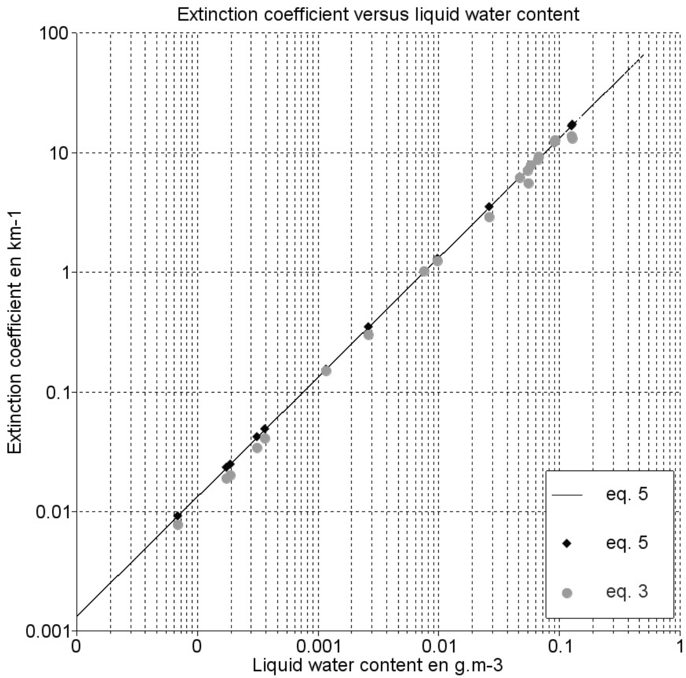

Fig. 3. Same as Fig. 2 for $\lambda = 11\,\mu m$.

AMTD
6, 9623–9653, 2013

Relationship between optical extinction and liquid water content in fogs

C. Klein and A. Dabas

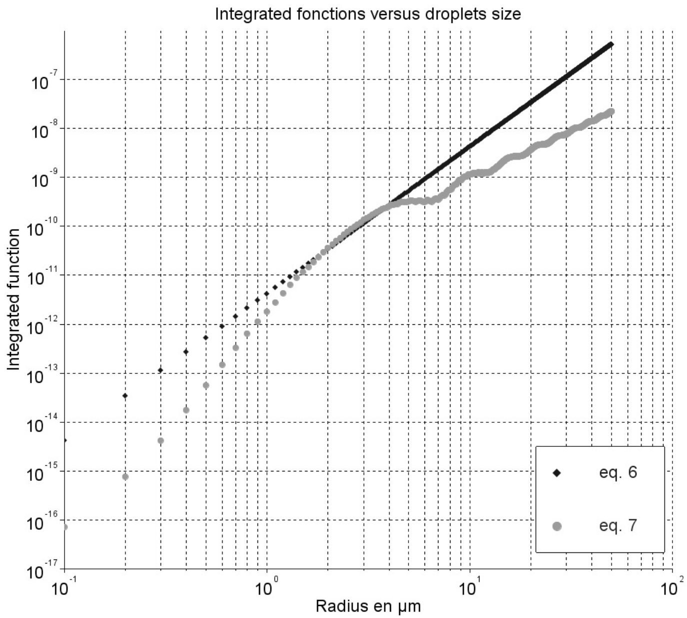

Fig. 4. Functions $F(r) = 4\pi\rho_{H_2O}r^3/3$ and $\hat{F}(r) = 4\rho_{H_2O}r^2Q_{ext}(r,\lambda)/(3c_e(\lambda))$ as a function of the droplet radius r for $\lambda = 4\,\mu m$.

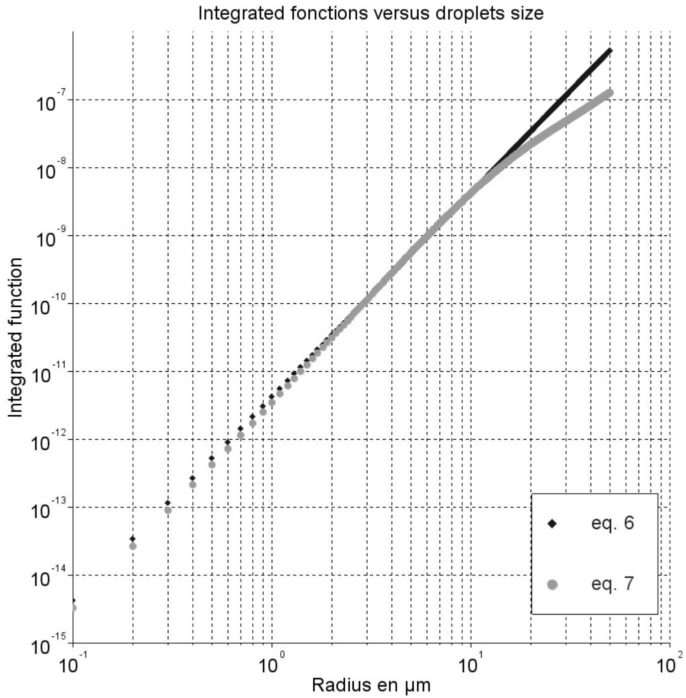

Fig. 5. Same as Fig. 4 for $\lambda = 11\,\mu m$.

AMTD
6, 9623–9653, 2013

Relationship between optical extinction and liquid water content in fogs

C. Klein and A. Dabas

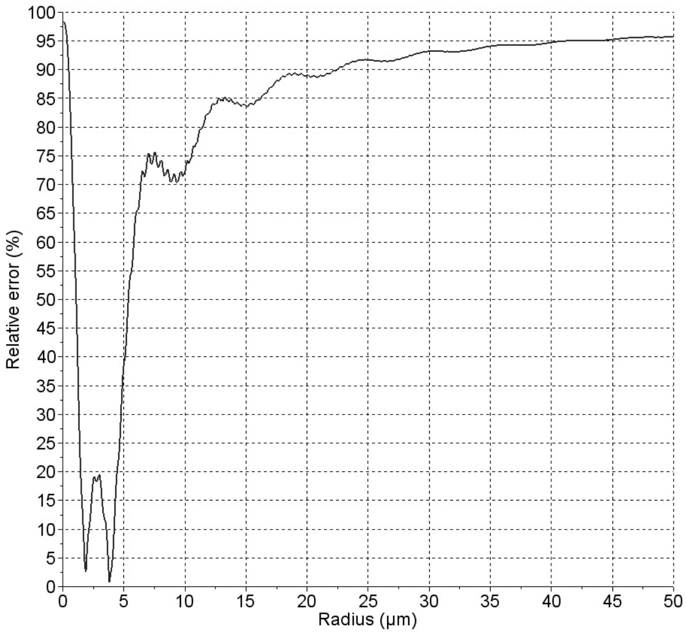

Fig. 6. Relative difference $|1 - \hat{F}/F|$ between $F(r)$ and $\hat{F}(r)$ (in %) for $\lambda = 4\,\mu m$.

AMTD
6, 9623–9653, 2013

Relationship between optical extinction and liquid water content in fogs

C. Klein and A. Dabas

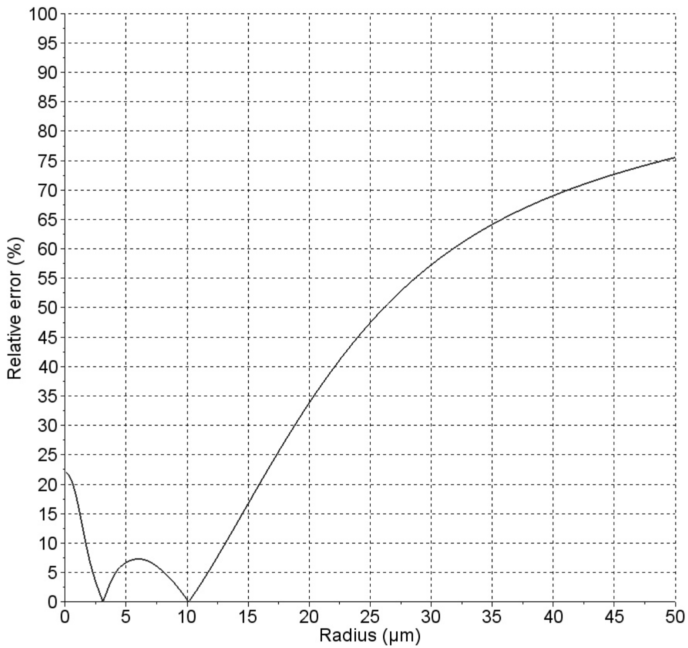

Fig. 7. Same as Fig. 6 for $\lambda = 11\ \mu m$.

AMTD
6, 9623–9653, 2013

Relationship between optical extinction and liquid water content in fogs

C. Klein and A. Dabas

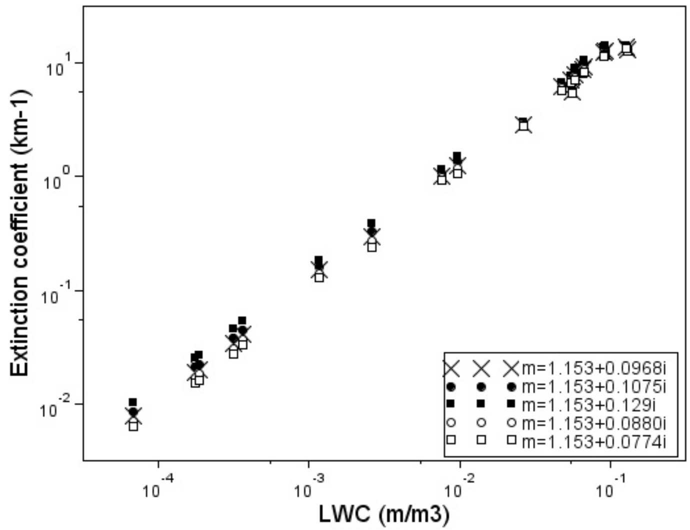

Fig. 8. Extinction coefficients (as a function of the liquid water content) for the 20 size distributions of PARISFOG for a refractive index with a variable imaginary part. The reference is the refractive index of water $m = 1.153 + 0.0968i$ (x). The circles and squares are for the refractive indices that produce maximum extinction efficiency relative errors of 10 and 25 % respectively, in excess (filled) or default (open).

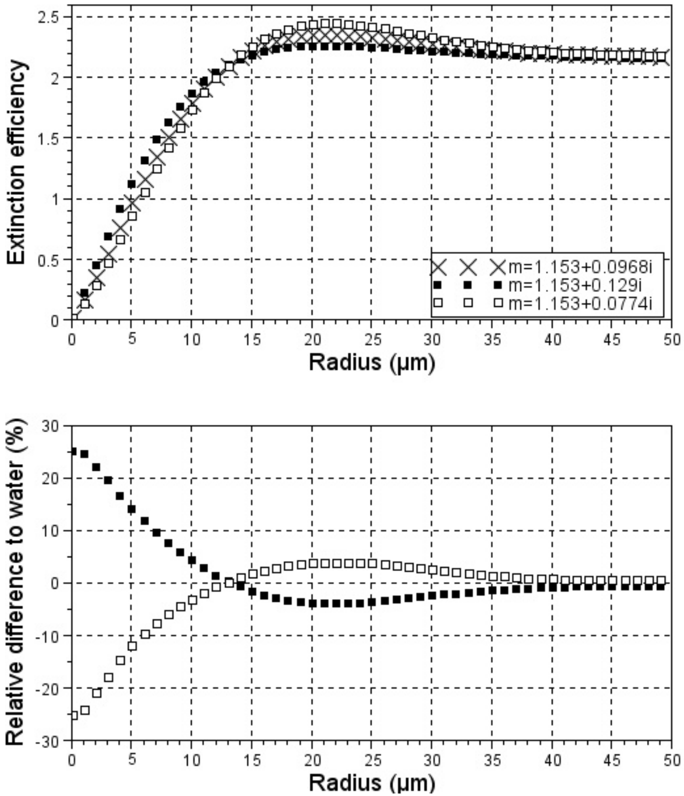

Fig. 9. Extinction efficiencies (top panel) for the refractive indices $m = 1.153 + i0.0968$ (water), $m = 1.153 + i0.129$ and $m = 1.153 + i0.0774$, and relative difference (in %) to pure water (bottom panel). The laser wavelength is 11 µm.

AMTD
6, 9623–9653, 2013

Relationship between optical extinction and liquid water content in fogs

C. Klein and A. Dabas

Title Page
Abstract | Introduction
Conclusions | References
Tables | Figures
◀| |▶
◀ ▶
Back | Close
Full Screen / Esc
Printer-friendly Version
Interactive Discussion

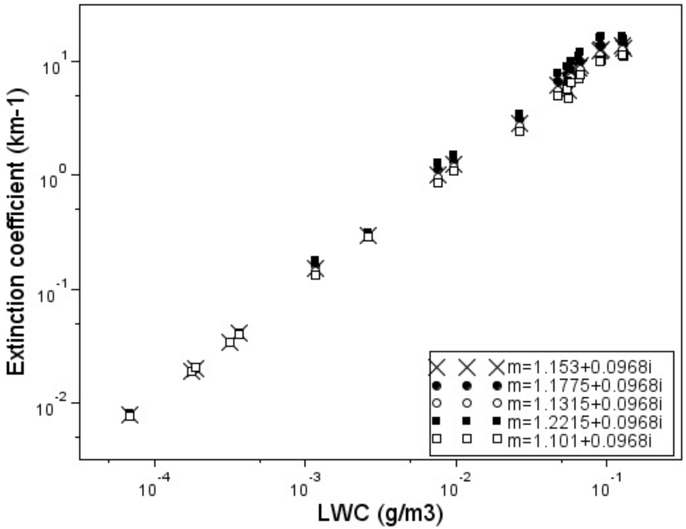

Fig. 10. Same as Fig. 8 for refractive indices with a variable real part.

AMTD
6, 9623–9653, 2013

Relationship between optical extinction and liquid water content in fogs

C. Klein and A. Dabas

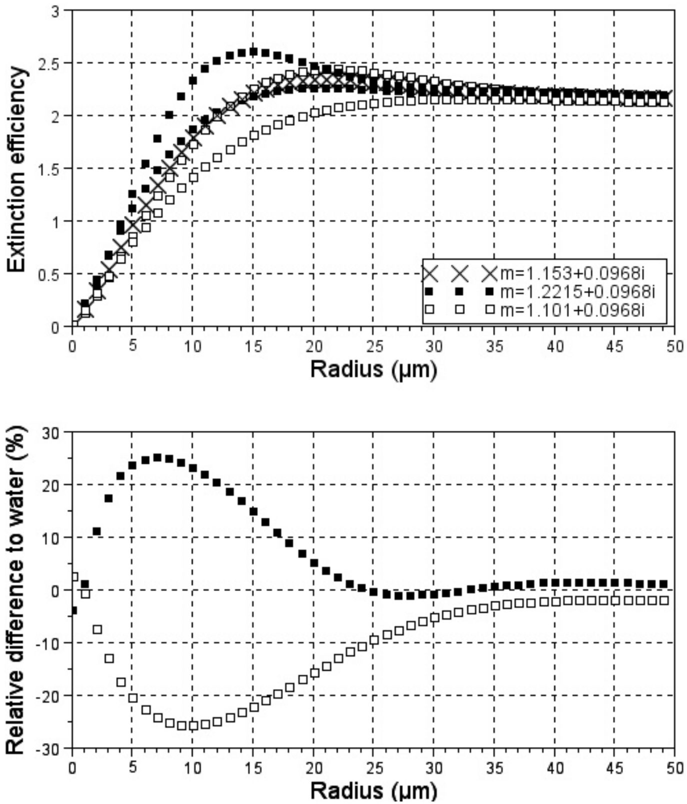

Fig. 11. Same as Fig. 9 for varying real parts of the fog droplet refractive index.

AMTD
6, 9623–9653, 2013

Relationship between optical extinction and liquid water content in fogs

C. Klein and A. Dabas

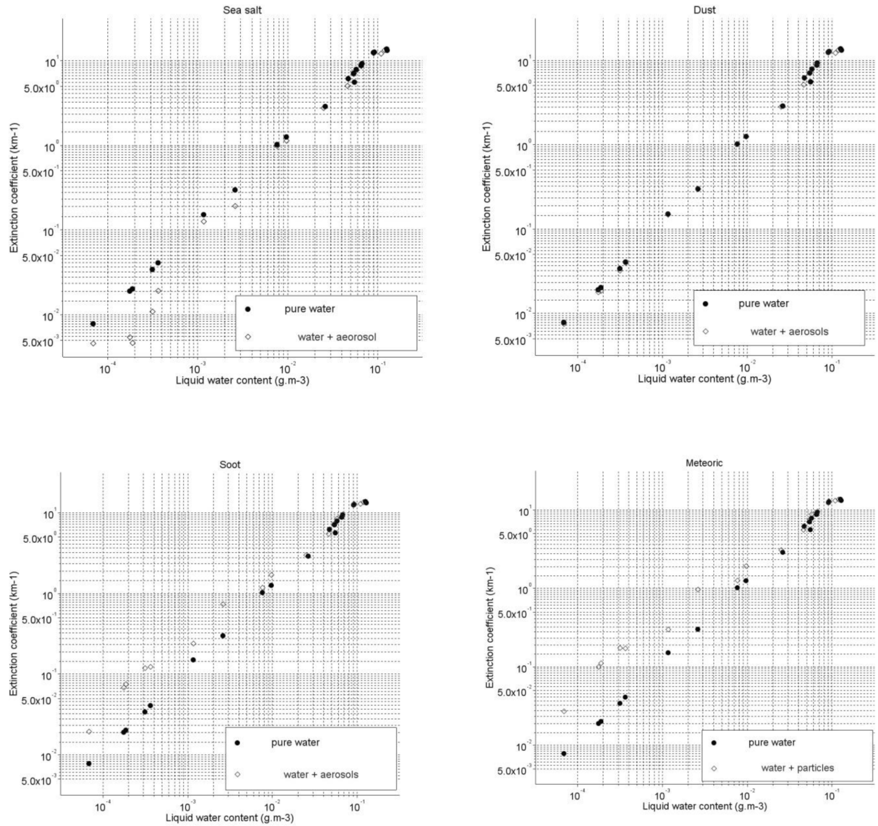

Fig. 12. Extinction coefficient vs. liquid water content for the 20 fog cases studied in the article and a refractive index for particles with radii < 1 µm equal to the refractive index of sea salt (top left panel), dust (top right panel), soot (bottom left panel) and meteoric particles (bottom right panel) according to Fenn et al. (1985) (see Table 2). The extinction coefficients (in pink) are compared to the extinction coefficients obtained with the refractive index of pure water at 11 µm.

AMTD
6, 9623–9653, 2013